ac electric-field-induced resonant energy transfer between cold Rydberg atoms

J. A. Petrus, P. Bohlouli-Zanjani, J. D. D. Martin

Department of Physics and Astronomy, University of Waterloo, Waterloo, ON, N2L 3G1, Canada

An oscillating electric field at 1.356 GHz was used to promote the resonant energy transfer process: $43d_{5/2}+43d_{5/2} \to 45p_{3/2}+41f$ between translationally cold ^{85}Rb Rydberg atoms. The ac Stark shifts due to this dressing field created degeneracies between the initial and final two-atom states of this process. The ac field strength was scanned to collect spectra which are analogous to dc electric-field-induced resonant energy transfer spectra. Different resonances were observed for different magnetic sublevels involved in the process. Compared to earlier work performed at higher frequencies, the choice of dressing frequency and structure of the spectra may be intuitively understood, by analogy with the dc field case.

I. INTRODUCTION

The interaction energies between neighbouring Rydberg atoms can be much larger than between ground state atoms, separated by the same distance. These interactions can be made even larger if they are resonant. For example, Vogt *et al.* [1] have demonstrated that optical transitions to Cs Rydberg states are partially inhibited by tuning the energy of two Cs atoms in the $38p_{3/2}$ state to be identical to the energy of a $38s_{1/2}$, $39s_{1/2}$ atom pair. This tuning was accomplished using small electric fields ($\approx 1 - 2$ V/cm). With this induced degeneracy, the electric dipole-dipole interaction gives a first order energy shift, rather than a weaker second-order effect (van der Waals).

The use of external fields to create resonant interactions is common in atomic physics. Tunable dc magnetic fields may be used to create Feshbach resonances, dramatically enhancing the interactions between ultracold atoms [2, 3]. Oscillating fields may also be used. For example, Gerbier *et al.* [4] recently demonstrated that oscillating magnetic fields may also be used to shift dressed state energy levels into resonance, and thereby enhance interatomic interactions between ultracold atoms. The ability to vary both the frequency and amplitude of the "dressing field" gives additional latitude in achieving the resonance condition.

In a similar vein, we have recently shown that the resonant energy transfer process:

$$43d_{5/2} + 43d_{5/2} \to 45p_{3/2} + 41f \qquad (1)$$
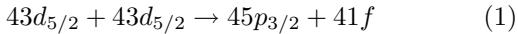
in ^{85}Rb may be greatly enhanced by the application of a microwave field (28.5 GHz) of appropriate field strengths [5]. The results agreed with the theoretical predictions for the ac Stark effect, but it is not obvious why 28.5 GHz was an appropriate frequency to use. Since all of the participating levels ($43d_{5/2}$, $45p_{3/2}$ and $41f$) show significant shifts at this frequency, the situation is complicated. In the present work, we demonstrate that a much lower frequency of 1.356 GHz – chosen to be slightly blue detuned from the $41f - 41g$ transition – shifts only $41f$ significantly. By varying the dressing field amplitude we can shift the process in Eq. 1 into resonance.

There is an additional benefit to using a lower dressing frequency. As discussed in Ref. [5], the different magnetic sublevels involved in Eq. 1 show different ac Stark shifts. With a 28.5 GHz dressing field, these give a complicated series of resonances. In the present work – at much lower frequencies – the spectra are not as complicated, as the only important magnetic sublevel structure is due to the $41f$ states.

II. THEORETICAL BACKGROUND

This section begins by motivating the choice of a dressing frequency of 1.356 GHz, and concludes by discussing the techniques used for calculating the dressed atom energy levels.

The process given in Eq. 1 is not resonant in the absence of applied fields. The final state is lower in energy than the initial state by approximately 10 MHz [5]. The $41f$ states shift to lower energy with increasing dc electric field. The other states involved have significantly smaller dc polarizabilities, and do not shift as much. Therefore, the resonant energy transfer process in Eq. 1 cannot be shifted into resonance with a dc field.

The shift of the $41f$ states to lower energies can be intuitively understood using 2$^{\text{nd}}$ order perturbation theory. For an arbitrary state $|\phi>$, and an electric field of magnitude $\varepsilon_{z,dc}$ pointing in the z direction:

$$\Delta E_\phi = \varepsilon_{z,dc}^2 \sum_{p \neq \phi} \frac{|<\phi|\mu_z|p>|^2}{(E_\phi - E_p)}, \qquad (2)$$

where E_p refers to the energy of state $|p>$ and μ_z is the electric dipole moment in the z direction. Figure 1a illustrates the simplified case of one dominant perturber. States are pushed away in energy from the perturber. For the $41f$ state, the dominant nearby perturber is the $41g$ state, located 1.19 GHz higher in energy. As an electric field is applied, the $41f$ state shifts down in energy, away from $41g$.

The expression for the perturbative ac Stark shift is

similar to that for the dc case:

$$\Delta E_\phi = \frac{1}{2}\varepsilon_{z,ac}^2 \sum_{p\neq\phi} \frac{(E_\phi - E_p)|<\phi|\mu_z|p>|^2}{(E_\phi - E_p)^2 - (\hbar\omega)^2}, \qquad (3)$$

where ω is the angular frequency of a dressing field, pointing in the z direction with electric field amplitude $\varepsilon_{z,ac}$. (For a derivation, see Ref. [6].) Again, Fig. 1b illustrates the simplified case of one dominant perturber. In contrast to the dc effect, ω may be used to control the sign of the shift. In our specific case of Rb, we expect that applying a dressing frequency greater than the $41f - 41g$ transition frequency would cause the $41f$ state to move up in energy with increasing dressing field strength. As we demonstrate experimentally in the Apparatus and Results section, this shifts the initial and final states of Eq. 1 into resonance.

Although the perturbative formula (Eq. 3) for the ac Stark shift provides insight, some caution is required in its application. In particular, the energy shifts of the $41f$ states that are required to make the process in Eq. 1 degenerate are of the same order of magnitude as the fine structure splitting between $41f_{5/2}$ and $41f_{7/2}$ levels (2.3 MHz). This was not as significant with a dressing field frequency of 28.5 GHz as the shifts of the $41f$ states were not as large (the $43d_{5/2}$ and $45p_{3/2}$ states shifted more to make up the energy difference in Eq. 1, and their fine structure splitting is much larger). To treat this complication the dressed energy levels are calculated using a Floquet approach [7]. This approach takes the "bare" basis states of energy E_{bi} and adds "sideband" states of energy $E_{bi} + k\hbar\omega$, where k is an integer. The ac field introduces coupling between states differing in sideband order k by one. Our basis set and couplings are very similar to those used in dc electric-field Stark map calculations [8]. These calculations use the experimentally determined ^{85}Rb Rydberg energy levels [9, 10] as input. A nice description of the Floquet approach is given in Ref. [11].

III. APPARATUS AND RESULTS

We start with a general overview of the experiment. To observe resonant energy transfer, we optically excite cold ^{85}Rb atoms from a magneto-optical trap (MOT) to Rydberg states using a pulse of light. Then a dc or ac electric field of variable amplitude is applied. The Rydberg atoms are allowed to interact in this field for a fixed amount of time, and then a selective field ionization pulse is applied to measure the Rydberg state populations. If, for example, $43d_{5/2}$ Rydberg states are excited and the ac field establishes the resonance condition between the initial and final states shown in Eq. 1, then both $45p_{3/2}$ and $41f$ Rydberg atoms are observed. By scanning the field strength, repeating the excitation and detection process, and recording the fraction of Rydberg atoms transferred to the $45p_{3/2}$ level, resonant energy transfer spectra may be obtained (Fig. 3b).
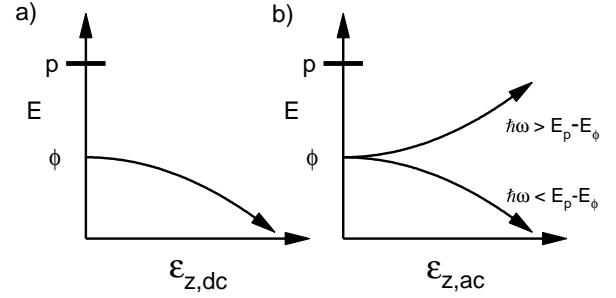

FIG. 1: (a) The dc Stark effect in the case of a single nearby perturber $|p>$. The energy of the perturbed state $|\phi>$ is shown as a function of the dc electric-field magnitude $\varepsilon_{z,dc}$. (b) The ac Stark effect in the case of a single nearby perturber $|p>$. In this case the shifts are shown as a function of the amplitude of the oscillating electric field $\varepsilon_{z,ac}$. These two figures illustrate that the ac Stark shift direction may be altered by an appropriate choice of frequency ω, whereas the dc Stark shift direction is fixed. In both cases the perturber also shifts with field strength; however, this has not been shown.
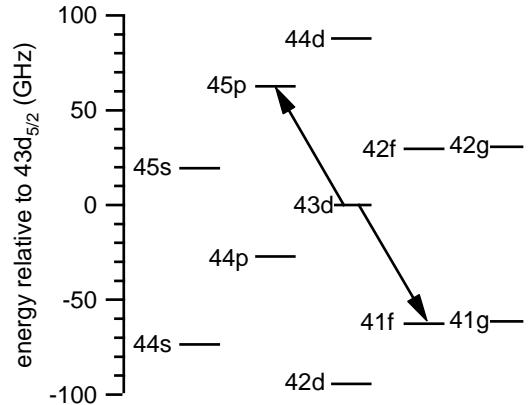

FIG. 2: Some relevant ^{85}Rb Rydberg atom energy levels. Fine structure is too small to be observed on this scale (e.g. $43d_{3/2}$ and $43d_{5/2}$). In addition, although the g and f series appear degenerate, $41g$ is approximately 1.19 GHz higher in energy than $41f$. The arrows indicate the transitions involved in the ac-electric-field assisted resonant energy transfer (see Eq. 1).

We will now discuss the various aspects of the experiment in more detail. The Rydberg atoms are excited using a two-colour scheme involving the 780 nm light used for cooling and trapping, and additional light at approximately 480 nm. This blue light is generated by frequency doubling a cw Ti:sapphire laser. It is introduced to the atoms in $1-2\mu$s pulses at a repetition rate of 10 Hz, using an acousto-optic modulator. Our frequency stabilization scheme for the Ti:sapphire laser has been discussed previously [12].

Approximately 25 ms prior to photoexcitation, the coil current generating the inhomogeneous magnetic field necessary for operation of the MOT is switched off. A 25 ms delay allows the fields due to eddy currents to decay. By using microwave spectroscopy of a magnetic-field-sensitive transition [13], we have verified that the residual magnetic field is less than 0.02 G at the time of photoexcitation. Following excitation, two parallel metal plates surrounding the atoms are used to apply both dc and ac fields. One-photon transitions may also be used to zero-out any residual electric field, and calibrate applied electric fields [14] (as required for dc electric field assisted resonant energy transfer spectra – see Fig. 3a).

Photoexcitation to Rydberg states takes place with no deliberately applied dc electric field. For dc-electric-field induced resonant energy transfer spectra, the field is ramped up over 160 ns, immediately following Rydberg excitation (ramping this up relatively slowly avoids ringing). In the case of ac-electric-field induced resonant energy transfer, the oscillating field is switched on approximately 3 μs following photoexcitation (a delay of this magnitude was not necessary, but it is important that the dressing field and laser excitation do not temporally overlap). The Agilent E8254A synthesizer providing this field has a specified rise time of 100 ns. These field conditions are maintained for approximately 20 μs, in which time the cold atoms can possibly change states due to the resonant energy transfer process (at our densities this time gives maximum amounts of transfer of about $10 - 30\%$). It is essential to switch off the ac field prior to selective field ionization. Otherwise, this normally non-resonant field is shifted into resonance with various transitions as the electric field increases, creating population transfer unrelated to interatomic interactions.

Selective field ionization allows the $nd_{5/2}$, $(n + 2)p_{3/2}$ and $(n - 2)f$ populations to be distinguished. All three signals are measured simultaneously using boxcar integrators, digitized and recorded as a function of dc or ac field strength.

To illustrate the similarities between ac- and dc-electric-field induced resonant energy transfer spectra, both have been collected (see Fig. 3). For the process:

$$nd_{5/2} + nd_{5/2} \rightarrow (n + 2)p_{3/2} + (n - 2)f \qquad (4)$$

the final state is higher in energy than the initial state for $n \geq 44$, allowing this process to be shifted into resonance with a dc electric field. In Ref. [5] an $n = 44$ spectrum was presented. Here in Fig. 3a we show the case of $n = 46$. There has been a previous report of this resonant energy transfer spectrum in the literature [15], but it differs from what we have observed, possibly due to differences in signal to noise. Note the excellent agreement between the calculated and observed resonance fields.

As discussed in the introduction, and shown experimentally in Ref. [5], dc fields cannot be used to shift the process in Eq. 4 into resonance at $n = 43$. However, as illustrated in Fig. 3b, an ac electric field at frequency of 1.356 GHz, approximately 160 MHz higher than the
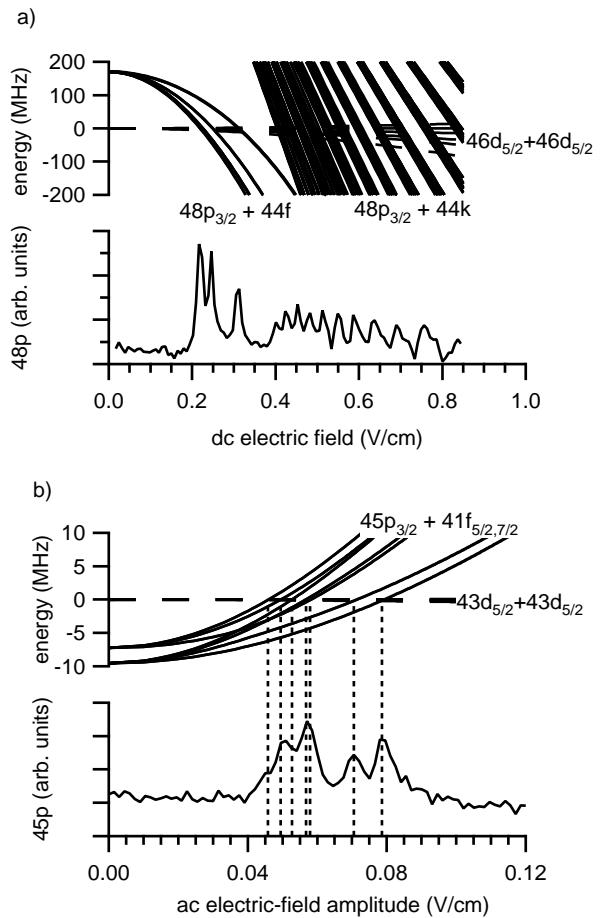

FIG. 3: (a) dc electric-field-induced resonant energy transfer: $46d_{5/2} + 46d_{5/2} \rightarrow 48p_{3/2} + 44f, 44k$. The $44k$ label refers to Stark states – in this case superpositions of angular momentum states with $\ell \geq 4$. (b) ac electric-field-induced resonant energy transfer: $43d_{5/2} + 43d_{5/2} \rightarrow 45p_{3/2} + 41f$, using a dressing frequency of 1.356 GHz. Note the different horizontal axis scalings for (a) and (b). Also shown are calculated total energies of initial and final state atom pairs (for different magnetic sublevel possibilities). The calculation procedures are discussed in the text. Vertical dashed lines are shown in (b) to highlight the agreement between the calculated and experimentally observed resonance field amplitudes.

$41f - 41g$ transition, raises the energy of the final state of Eq. 4, allowing the resonance condition to be achieved. The choice of 1.356 GHz is somewhat arbitrary. The frequency of the ac field should be far enough off resonance to avoid population transfer, but not so far that unreasonably strong field amplitudes are required.

Due to unknown impedance mismatchs, we cannot readily determine the applied ac field strength electrically. To calibrate the applied ac electric field amplitude in Fig. 3b we observed microwave spectra of the single-photon $43d_{5/2}$ to $41f_{5/2,7/2}$ transitions in the presence of a 1.356 GHz dressing field. These were done at low density to avoid interatomic effects. A comparison of

observed and expected shifts (calculated using the Floquet approach) allowed us to assign field strengths to synthesizer power levels. As we also use this calculation to predict the resonance field strengths, we cannot attach much significance to the overall absolute agreement between the observed and calculated resonance fields in Fig. 3b. However, the simultaneous agreement of several resonance peaks (corresponding to different magnetic sub-level possibilities) suggests that the calculation is correct, as we only used the shift of the $m_j = 1/2$ states for the field strength calibration.

Some practical advantages of applying a relatively low frequency field (1.356 GHz here *vs.* 28.5 GHz in Ref. [5]) are that the resulting field homogeneity can be much larger due to the longer corresponding radiation wavelength, and that sources of lower RF frequencies are more readily available.

IV. DISCUSSION

We have shown that ac electric fields may be used to induce resonant energy transfer in a conceptually similar manner as dc electric fields. This method for enhancing the interactions between Rydberg atoms may be useful for "dipole-blockade" [16]. Local blockade has been achieved through use of the van der Waals interaction between Rydberg atoms [17, 18] (See also Ref. [19] for progress on very small numbers of interacting atoms.) However, it is desirable to enhance the interatomic interactions by making them resonant. This has recently been achieved using dc electric fields [1]. The ac Stark shifts induced by dressing fields offer an additional means to accomplish this with possible distinct advantages. For example in a glass cell (coated with alkali) it is typically difficult to establish dc electric fields with external electrodes, whereas high frequency ac fields can be applied more easily (see, for example, Ref. [20]).

Atomic energy levels may be determined by dc field induced resonant energy transfer spectra (see, for example, Ref. [14]). The ac field induced resonant energy transfer process may also be useful in this context. In this and other applications the frequency of the applied fields allows a variability in the signs and magnitudes of the Stark shifts involved that gives more flexibility than the dc shift alone.

[1] T. Vogt, M. Viteau, J. Zhao, A. Chotia, D. Comparat, and P. Pillet. Dipole blockade at Förster resonances in high resolution laser excitation of Rydberg states of cesium atoms. *Phys. Rev. Lett.*, 97:083003, 2006.

[2] S. Inouye, M. R. Andrews, J. Stenger, H.-J. Miesner, D. M. Stamper-Kurn, and W. Ketterle. Observation of Feshbach resonances in a Bose-Einstein condensate. *Nature*, 392:151, 1998.

[3] Ph. Courteille, R. S. Freeland, D. J. Heinzen, F. A. van Abeelen, and B. J. Verhaar. Observation of a Feshbach resonance in cold atom scattering. *Phys. Rev. Lett.*, 81(1):69–72, Jul 1998.

[4] F. Gerbier, A. Widera, S. Fölling, O. Mandel, and I. Bloch. Resonant control of spin dynamics in ultracold quantum gases by microwave dressing. *Phys. Rev. A*, 73:041602, 2006.

[5] P. Bohlouli-Zanjani, J. A. Petrus, and J. D. D. Martin. Enhancement of Rydberg atom interactions using ac Stark shifts. *Phys. Rev. Lett.*, 98:203005, 2007.

[6] M. Haas, U. D. Jentschura, and C. H. Keitel. Comparison of classical and second quantized description of the dynamic Stark shift. *Am. J. Phys.*, 74:77, 2006.

[7] Jon H. Shirley. Solution of the Schrödinger equation with a Hamiltonian periodic in time. *Phys. Rev.*, 138(4B):B979–B987, May 1965.

[8] M. L. Zimmerman, M. G. Littman, M. M. Kash, and D. Kleppner. Stark structure of the Rydberg states of alkali metal atoms. *Phys. Rev. A*, 20:2251, 1979.

[9] W. Li, I. Mourachko, M. W. Noel, and T. F. Gallagher. Millimeter-wave spectroscopy of cold Rb Rydberg atoms in a magneto-optical trap: Quantum defects of the ns, np and nd series. *Phys. Rev. A*, 67:052502, 2003.

[10] J. Han, Y. Jamil, D. V. L. Norum, P. J. Tanner, and T. F. Gallagher. Rb nf quantum defects from millimeter-wave spectroscopy of cold ^{85}Rb Rydberg atoms. *Phys. Rev. A*, 74:054502, 2006.

[11] W. van de Water et al. Microwave multiphoton and excitation of helium Rydberg atoms. *Phys. Rev. A*, 42:572–591, 1990.

[12] P. Bohlouli-Zanjani, K. Afrousheh, and J. D. D. Martin. Optical transfer cavity stabilization using current-modulated injection-locked diode lasers. *Rev. Sci. Instrum.*, 77:093105, 2006.

[13] K. Afrousheh et al. Resonant electric dipole-dipole interactions between cold Rydberg atoms in a magnetic field. *Phys. Rev. A*, 73:063403, 2006.

[14] K. Afrousheh, P. Bohlouli-Zanjani, J. A. Petrus, and J. D. D. Martin. Determination of the ^{85}Rb ng-series quantum defect by electric-field-induced resonant energy transfer between cold Rydberg atoms. *Phys. Rev. A*, 74:062712, 2006.

[15] M. Reetz-Lamour et al. Prospects of ultracold Rydberg gases for quantum information processing. *Fortschr. Phys.*, 54:776, 2006.

[16] M. D. Lukin et al. Dipole blockade and quantum information processing in mesoscopic atomic ensembles. *Phys. Rev. Lett.*, 87:037901, 2001.

[17] D. Tong et al. Local blockade of Rydberg excitation in an ultracold gas. *Phys. Rev. Lett.*, 93:063001, 2004.

[18] T. Cubel Liebisch, A. Reinhard, P. R. Berman, and G. Raithel. Atom counting statistics in ensembles of interacting Rydberg atoms. *Phys. Rev. Lett.*, 95:253002, 2005.

[19] T. A. Johnson et al. Rabi oscillations between ground and Rydberg states with dipole-dipole atomic interactions. *Phys. Rev. Lett.*, 100:113003, 2008.

[20] A. K. Mohapatra, T. R. Jackson, and C. S. Adams. Coherent optical detection of highly excited Rydberg states using electromagnetically induced transparency. *Rev. Lett.*, 98:113003, 2007.